Development and Validation of Fluorescence Spectroscopic Assays to Evaluate Antioxidant Efficacy. Application to Metal Chelators

Arti Arora and Gale M. Strasburg*

Department of Food Science and Human Nutrition, Michigan State University, East Lansing, Michigan 48824

ABSTRACT: Two fluorescence-based assays were developed for rapid evaluation of compounds for antioxidant activity. These assays were based on the quenching of intensity of the fluorescent probe and an increase in its fluorescence anisotropy due to the free radicals generated during lipid peroxidation. A large unilamellar vesicle system, containing the fluorescence probe diphenylhexatriene–propionic acid, was used to study the effects of chelators on metal-ion-induced lipid peroxidation. In this paper, the actions of the chelating agents ethylenediaminetetraacetic acid disodium salt (EDTA), nitrilotriacetic acid trisodium salt (NTA), adenosine-5′-diphosphate disodium salt (ADP), and sodium citrate on Fe(II)- and Fe(III)-induced peroxidation were compared. The effects of chelators on metal-ion-induced peroxidation depended on the type of metal used to initiate peroxidation and, for citrate, also on the concentration of chelator used. EDTA strongly suppressed both Fe(II)- and Fe(III)-induced peroxidation in this system. NTA and ADP inhibited Fe(III)-induced peroxidation but enhanced Fe(II)-induced peroxidation at all concentrations tested. Citrate promoted both Fe(II)- and Fe(III)-induced peroxidations at lower chelator-to-metal ratios; however, at higher ratios, it inhibited both peroxidations. The results of the two fluorescence-based assays agreed well with the quantitation of conjugated dienes and hydroperoxides by high-performance liquid chromatography. The combination of sensitivity, speed, and general utility associated with these methods suggests that these methods will be useful in rapid screening of extracts and purified compounds for antioxidant activity.

JAOCS 74, 1031–1040 (1997).

KEY WORDS: Antioxidants, chemiluminescence, diphenylhexatriene–propionic acid, fluorescence spectroscopy, free radicals, hydroperoxides, lipid peroxidation, liposomes, membrane fluidity, metal chelators.

The peroxidation of lipids *via* uncontrolled free-radical chain reactions is a critically important reaction in physiological and toxicological processes in human health and disease, as well as in the stability of food products during storage (1). In biomembranes, it leads to a disruption in structure and a loss of protective function (2).

*To whom correspondence should be addressed.
E-mail: stragale@pilot.msu.edu.

Membrane lipid peroxidation is greatly stimulated by the presence of transition metals, through enhancement of initiation reactions, as well as through metal ion catalysis of lipid hydroperoxide decomposition reactions (3). Chelators can alter the rate of metal-catalyzed peroxidation by steric effects, variations in redox potentials, and alterations in solubility properties of the metal (4). Several studies have been conducted to determine the effects of metal chelators on lipid peroxidation (5–10); however, the effects are complicated and not fully understood (7).

The choice of model system and the methods used in the study of lipid peroxidation often introduce artifacts that complicate interpretations of the results. Results from many commonly used model systems, such as methyl linoleate micelles, may have little relationship to food products because they are not structurally representative of membrane phospholipids or triglycerides (11). Sarcoplasmic reticulum microsomes (12–14) and mammalian erythrocyte membranes (15,16) are useful models in membrane peroxidation studies. However, use of biological membranes as lipid substrates to evaluate antioxidant activity of compounds is complicated by the presence of numerous endogenous prooxidative and antioxidative factors, including transition metals, heme proteins, catalases, glutathione reductase, and superoxide dismutase (17–20). Although biological membranes may provide useful information on oxidative damage or antioxidant status in an individual, the inherent variability from preparation to preparation makes their use less attractive as systems for evaluation of antioxidant activity of compounds or plant extracts.

As an alternative model to study lipid peroxidation, artificial membranes such as liposomes offer clear advantages over biological membranes. In particular, large unilamellar vesicles (LUV) of a defined lipid composition constitute a simple and convenient system for studying lipid peroxidation and its inhibition by antioxidants without the ambiguities introduced by enzymes or scavengers that may be present in more complex biological systems (21).

Use of a defined lipid substrate and structure, coupled with fluorescence spectroscopy, offers the inherent advantages of speed, simplicity, and sensitivity for probing membrane structure. This methodology can be readily adapted to peroxida-

tion studies on the mechanism of action and efficacy of food antioxidants (22). The objective of this study was to develop a sensitive, quantitative, and rapid fluorescence-based assay for measuring lipid peroxidation and to apply the assay to evaluate antioxidant efficacy. LUV with the fluorescent probe 3-[*p*-(6-phenyl)-1,3,5-hexatrienyl]phenylpropionic acid (DPH–PA) were used to study the modulation of Fe(II)-, Fe(III)-, and Cu(II)-induced membrane peroxidation by the chelators disodium ethylenediaminetetraacetic acid (EDTA), nitrilotriacetic acid trisodium salt (NTA), adenosine-5′-diphosphate disodium salt (ADP), and sodium citrate. Results from these experiments were correlated with data obtained by measurement of conjugated dienes and the direct quantitation of hydroperoxides by high-performance liquid chromatography (HPLC)–chemiluminescence to validate the fluorescence-based assays.

EXPERIMENTAL PROCEDURES

Materials. Synthetic 1-stearoyl-2-linoleoyl-*sn*-glycero-3-phosphocholine (SLPC) of greater than 99% purity in chloroform solution was purchased from Avanti Polar Lipids (Alabaster, AL). The purity of the lipid was confirmed by thin-layer chromatography with two different solvent systems (chloroform/methanol/water, 65:25:4; chloroform/methanol/ammonium hydroxide, 65:25:4). The lipids were stored in amber glass vials, layered with nitrogen, sealed with Teflon tape, and stored at −20°C. The fluorescent probe DPH–PA was purchased from Molecular Probes (Eugene, OR). ADP, NTA, 3-[*N*-morpholino] propanesulfonic acid (MOPS), potassium tetraborate, cytochrome c from horse heart (prepared without trichloroacetic acid), 5-amino-2,3-dihydro-1,4-phthalazinedione (luminol), Chelex 100, methylene blue, and xylenol orange were from Sigma Chemicals (St. Louis, MO). 4-[2-Hydroxyethyl]-1-piperazine ethanesulfonic acid was purchased from Boehringer Mannheim (Indianapolis, IN). EDTA, $FeCl_3 \cdot 6H_2O$, $FeCl_2 \cdot 4H_2O$, and sodium phosphate were from Mallinckrodt (Paris, KY); citric acid monohydrate was from Fisher Scientific (Fair Lawn, NJ); and $CuCl_2 \cdot 2H_2O$ was from J.T. Baker (Phillipsburg, NJ). All glassware used in the study was acid-washed. Contaminating transition metals were removed from the sodium citrate, sodium chloride, and buffer stock solutions by maintaining the solutions in Chelex 100 (5 g/100 mL, wt/vol). The solutions were sparged with nitrogen prior to use. The metal solutions were made up fresh in nitrogen-sparged water immediately before use and stored on ice. The sodium citrate and ADP stock solutions were adjusted to a pH of 7.0.

Preparation of large unilamellar vesicles. LUV were prepared immediately before use according to the procedure outlined by MacDonald *et al.* (23) with a few modifications. Briefly, the lipid and fluorescent probe stocks, dissolved in chloroform and *N,N*-dimethylformamide respectively, were dried under vacuum onto the wall of a round-bottomed flask on a rotary evaporator. The mole ratio of fluorescent probe to lipid was maintained at 1:350. The lipid film obtained by evaporation was maintained under vacuum for at least an additional 0.5 h to remove any residual solvent, hydrated at a 10 mM lipid and 29 μM probe concentration in 500 μL of a solution that contained NaCl (0.15 M), MOPS (pH 7.0) (0.01 M) and EDTA (0.1 mM) for 30 min at a temperature at least 10°C higher than the transition temperature of the lipid (−16.2°C), and freeze-thawed 10 times in a solid carbon dioxide/ethanol bath. The resulting multilamellar vesicles were passed 29 times through 100-nm polycarbonate filters in a Liposofast extruder apparatus (Avestin, Ottawa, Canada). The LUV were characterized by freeze-fracture studies with a scanning electron microscope as described by MacDonald *et al.* (23).

Fluorescence experiments. For kinetic measurements, a 20-μL aliquot of the liposome suspension was diluted to 2 mL in buffer that contained 100 mM NaCl and 50 mM Tris-HEPES (pH 7.0) to achieve final concentrations of 100 μM lipid and 0.29 μM DPH–PA. The suspension was pre-incubated at room temperature for 5 min with continuous magnetic stirring to incorporate oxygen into the experimental system. Another 5-min incubation was done in the cuvette for temperature equilibration. An aliquot of the stock solution of the chelator to be tested was added to achieve the desired final concentration in the cuvette. Peroxidation was initiated by the addition of 20 μL of a 100-μM stock metal ion solution to achieve a final metal concentration of 1 μM. The control sample did not contain either added metal ions or chelator. The reaction was monitored over 21 min with readings being taken at 0 min, 1 min, and every 3 min thereafter.

Cuvette temperature was maintained at 22°C with a circulating water bath. The cuvette holder was also fitted with a magnetic stirring mechanism to maintain a well-dispersed suspension of vesicles. Fluorescence experiments were conducted in an SLM Instruments Model 4800 spectrofluorometer (Urbana, IL), interfaced to a computer with data acquisition hardware from On-Line Instrument Systems (Bogart, GA). The samples were excited with polarized light at 384 nm (slit width 2 nm), and vertical and horizontal components of the sample fluorescence, $I_{\parallel}$ and $I_{\perp}$, emitted through optical filters (KV 418; Schott, Duryea, PA), were detected in the T-format. The steady-state anisotropy, r_s, was calculated as:

$$r_s = (I_{\parallel} - I_{\perp}) / (I_{\parallel} + 2\, I_{\perp}) \qquad [1]$$

where $I_{\parallel}$ and $I_{\perp}$ are the fluorescent intensities of the vertically ($\parallel$) and horizontally ($\perp$) polarized emission when the sample is excited with vertically polarized light (24). Light scattering by the vesicle suspension was determined by measuring intensity in the absence of fluorescent probe, while using vertically polarized excitation light with the emission polarizer set to 55°. The ratio of this signal to that determined for membranes containing the probe gave the fraction of signal that resulted from light scattering. The light-scattering fraction was negligible relative to the fluorescence signal, and no corrections were made to the anisotropy values.

Preparation of SLPC hydroperoxides. SLPC hydroperox-

ides were prepared according to the procedure described by Miyazawa *et al.* (25) and modified by Zhang *et al.* (26). Twenty-five milligrams of lipid, dissolved in 25 mL of methanol that contained 0.1 mM methylene blue, were placed in a 250-mL beaker, cooled with ice water, and photoirradiated with two 150-watt lamps for 8 h. After photooxidation, the methylene blue was removed from the solution by solid-phase sequential extraction through two Supelclean LC-Si 6-mL, 1-g columns (Supelco, Bellefonte, PA). The resulting hydroperoxide-containing solutions were placed in amber glass vials (Avanti Polar Lipids), layered with nitrogen, sealed with Teflon tape, and maintained at −80°C until use. The concentration of hydroperoxides was determined by the xylenol orange assay developed by Jiang *et al.* (27).

HPLC–chemiluminescence assay and conjugated diene determination. LUV (2 mM) were suspended in 100 mM NaCl and 50 mM Tris-HEPES (pH 7.0). Oxidation was initiated with or without addition of chelator to a final concentration of 400 μM, followed by addition of Fe(II) ions to a final concentration of 200 μM. The reaction mixture of a total volume of 2.5 mL was maintained at 22°C throughout the experiment. Aliquots of 500 μL were removed at 0 min, 1 min, and at 30-min intervals thereafter, during the 90-min experiment. Lipid was extracted from the LUV suspension by adding 3 vol of ice-cold chloroform/methanol (2:1, vol/vol). The suspension was vortexed for 1 min and centrifuged at $750 \times g$ for 10 min, and the lower chloroform layer was collected. The extraction procedure was repeated twice. The chloroform fractions were combined, dried under nitrogen, immediately resuspended in mobile phase, and analyzed by HPLC–chemiluminescence with a normal-phase Supelcosil LC-NH_2 (5 μm, 250 × 4.6 mm) column with a Supelguard LC-NH_2 guard column (Supelco). The mobile phase, consisting of a 90:10 (vol/vol) solution of methanol and 10 mM sodium phosphate monobasic buffer, was adjusted to a final pH of 6.5 and was used at a flow rate of 1 mL/min with continuous helium sparging. A Waters 991 photodiode array detector (PDA) (Milford, MA), set at a range of 200–240 nm, was used to detect the shift from unconjugated diene absorption at 205 nm to conjugated diene absorption at 234 nm.

The eluate passing through the PDA detector was mixed with a chemiluminescence reagent at a postcolumn mixing tee. The luminescence reagent was prepared as described by Miyazawa *et al.* (25). It consisted of cytochrome c (10 μg/mL) and luminol (1 μg/mL), dissolved in 50 mM nitrogen-sparged borate buffer (pH 10.0) that contained 1% methanol to improve mixing with the mobile phase. The reagent was prepared daily, placed in amber glass containers, degassed, and continuously sparged with helium. The flow rate of the reagent was 1 mL/min. The chemiluminescence generated by the presence of hydroperoxides was detected by a Waters 474 fluorescence detector. The peak areas of the prepared standards, chromatographed under the same conditions as the samples, were used to construct the calibration curves. Separate calibration curves were generated for the quantitation of conjugated dienes and the hydroperoxides.

RESULTS

Characterization of the LUV. Figure 1 consists of electron micrographs of replicas of LUV that were slam-frozen, fractured, and shadowed. The micrograph in Figure 1A confirms that virtually all vesicles formed by extrusion contained single bilayers, a critical feature of our experimental system. Figure 1B illustrates the relatively homogeneous size distribution of the vesicles. The average diameter of the LUV was 80 nm.

DPH–PA fluorescence properties in the LUV. Initial experiments were conducted to determine the optimal concentrations of DPH–PA and the ratio of probe to phospholipid to be used in the LUV. DPH–PA had negligible fluorescence in the absence of phospholipids (Fig. 2A). Fluorescence intensity increased and reached saturation at 100 μM phospholipid, as increasing amounts of LUV were added to a fixed concentration of DPH–PA. The anisotropy values were stable over the phospholipid concentration range of 20–125 μM. When the

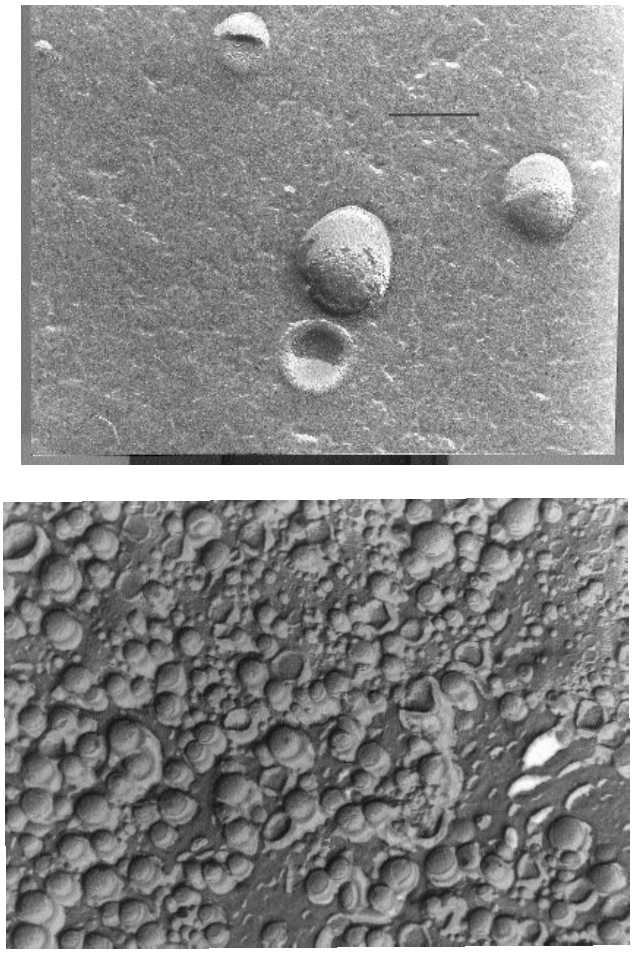

FIG. 1. Freeze-fracture electron micrographs of the large unilamellar vesicles (LUV) at a 10-mM concentration in a solution of 0.15 M NaCl, 0.01 M 3-[*N*-morpholino]propanesulfonic acid (pH 7.0) and 0.1 mM ethylenediaminetetraacetic acid (EDTA). The lengths of the bars represent 100 nm. These micrographs confirm the unilamellar nature of the vesicles (A) and their relatively homogeneous size distribution (B).

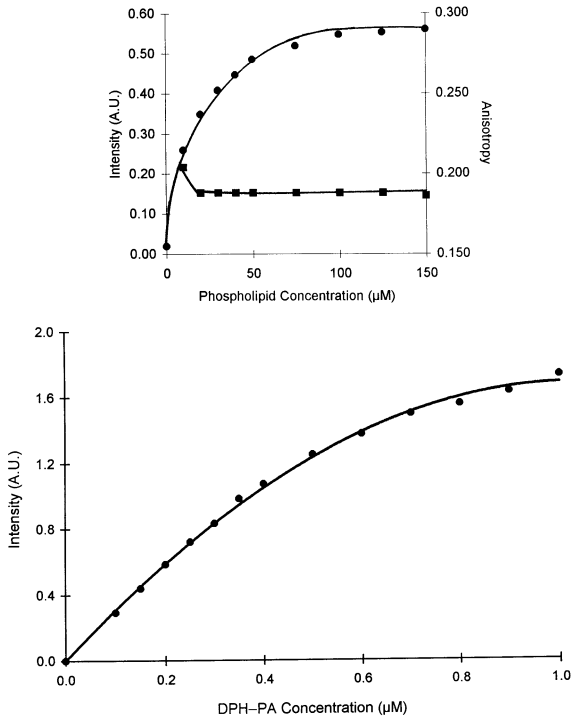

FIG. 2. Fluorescence intensity (●) and anisotropy (■) of diphenylhexatriene–propionic acid (DPH–PA) in LUV as a function of concentration. (A) 2 mL of buffer (100 mM NaCl/50 mM Tris-4-[2-hydroxyethyl]-1-piperazine ethanesulfonic acid, pH 7.0) containing 0.29 μM DPH–PA and various concentrations of phospholipid; and (B) 2 mL of buffer containing 100 μM phospholipid and various concentrations of DPH–PA. See Figure 1 for other abbreviation.

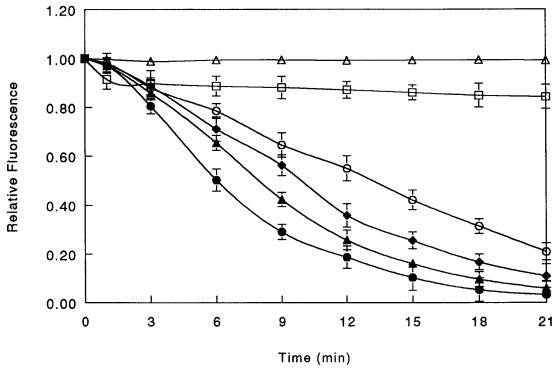

FIG. 3. Peroxidation of 100 μM 1-stearoyl-2-linoleoyl-*sn*-glycerol-3-phosphocholine (SLPC) LUV induced by 1 μM Fe(II) and 2 μM chelator. The rate of peroxidation was monitored by a decrease in fluorescence intensity as a function of time, as described in the Experimental Procedures section. Relative fluorescence on the y-axis represents the ratio of fluorescence intensity after a given time of oxidation vs. initial fluorescence intensity at time = 0 min. Values represent the mean ± standard deviation of triplicate measurements; △, control; ○, Fe(II); □, Fe(II)-EDTA; ◆, Fe(II)-adenosine-5′-diphosphate disodium salt (ADP); ▲, Fe(II)-nitrilotriacetic acid trisodium salt (NTA); ●, Fe(II)-citrate. See Figure 1 for other abbreviations.

phospholipid concentration was held constant at 100 μM (Fig. 2B), the fluorescence intensity increased linearly with the concentration of DPH–PA at lower concentrations. Above a concentration of 0.4 μM DPH–PA, the increase in fluorescence became nonlinear, though saturation was not observed at the probe concentrations tested. In all subsequent experiments, concentrations of 0.29 μM DPH–PA and 100 μM phospholipid were used. Under these conditions, the fluorescence intensity of DPH–PA was a linear function of its concentration in the membrane, and the lowest possible probe-to-lipid ratio was used, while maintaining a strong fluorescence signal.

Fe(II)-induced peroxidation monitored by fluorescence intensity decay. Figure 3 illustrates the effects of chelators on the rates of Fe(II)-induced peroxidation in the LUV, studied at a 2:1 molar ratio of chelator to metal. The rate of peroxidation was monitored by quenching the fluorescence intensity of the probe by the free radicals generated during lipid peroxidation. The control LUV with DPH–PA showed stable intensity values over the 21-min time period, indicative of the stability of the probe in the absence of initiators of peroxidation. When Fe(II) ions were added to initiate peroxidation in the vesicles, the fluorescence intensity decreased to approximately 30% of the original value by the end of the 21-min assay. Addition of EDTA, followed by Fe(II) ions, resulted in only a small decrease in fluorescence intensity values of the probe, indicating that EDTA behaved as an antioxidant under these conditions. However, the other three chelators studied—ADP, NTA, and citrate—acted as prooxidants, as evidenced by a more rapid drop in fluorescence intensity of the probe than that observed with the Fe(II) ions alone. When the chelators were added to the LUV in the absence of metal ions, there was no change in fluorescence intensity values (data not shown).

Fe(II)-induced peroxidation monitored by increase in fluorescence anisotropy. Fluorescence anisotropy was used to monitor the change in membrane fluidity that accompanied peroxidation (Fig. 4). Membrane peroxidation in the LUV was accompanied by an increase in the steady-state anisot-

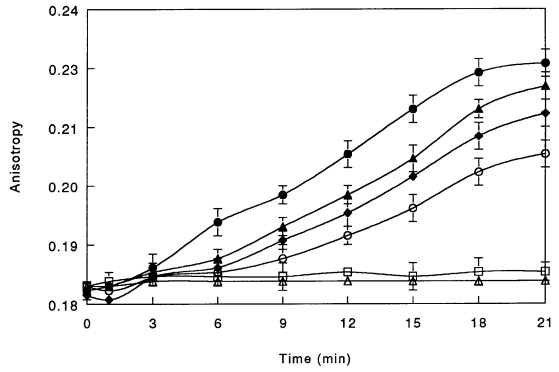

FIG. 4. Peroxidation of 100 μM SLPC LUV induced by 1 μM Fe(II) and 2 μM chelator. The rate of peroxidation was followed by an increase in fluorescence anisotropy as a function of time, as described in the Experimental Procedures section. Values represent the mean ± standard deviation of triplicate measurements; △, control; ○, Fe(II); □, Fe(II)-EDTA; ◆, Fe(II)-ADP; ▲, Fe(II)-NTA; ●, Fe(II)-citrate. See Figures 1 and 3 for abbreviations.

ropy parameter for DPH–PA. This increase in anisotropy, indicating a reduction of DPH–PA mobility in the lipid bilayer and a decrease in membrane fluidity, may be attributed to an increase in the molecular order of the fatty acyl chains in the bilayer (12).

The fluorescent anisotropy values for the control LUV were stable over the course of the assay, indicative of a membrane of unchanging fluidity. Similarly, there was no significant change in anisotropy in the LUV in the presence of the EDTA–Fe(II) complex at a 2:1 molar ratio. However, the chelators ADP, NTA and citrate, when complexed to Fe(II), all caused a greater increase in anisotropy values than did the Fe(II) ions alone, indicating a substantial loss of membrane fluidity upon peroxidation. These results were consistent with the time course of the loss of fluorescence intensity upon peroxidation observed in Figure 3.

Fe(III)-induced peroxidation of LUV. From either the decrease in fluorescence intensity (Fig. 5) or the increase in anisotropy (Fig. 6) to monitor the progress of membrane peroxidation, Fe(III) ions were less effective than Fe(II) ions in inducing peroxidation in the LUV. Furthermore, the effects of chelators on the rate of Fe(III)-induced lipid peroxidation were different from the Fe(II)-induced peroxidation in the LUV. Of all chelators examined, only the citrate–Fe(III) complex acted as a prooxidant. EDTA, ADP, and NTA all acted as antioxidants in the presence of Fe(III) ions, as indicated by the reduction in fluorescence intensity decline (Fig. 5) or by the smaller increase in anisotropy values (Fig. 6) compared to the results obtained with Fe(III) alone.

Cu(II)-induced peroxidation of LUV. Under the assay conditions employed in this study, neither Cu(II) ions alone (present in the upper, nonreductive state) nor Cu(II) ions complexed with chelators initiated peroxidation in the vesicles (data not shown).

Effect of chelator concentrations. For the chelators that exhibited a prooxidant effect in the presence of Fe (II) or Fe(III) ions at the initial molar ratios of 2:1 tested, the effects of varying the concentration of chelators relative to the metal ions were also examined. Figure 7A shows the effects of a 1:1, 5:1, 10:1, and 20:1 molar ratio of NTA relative to Fe(II) on rates of peroxidation. NTA maintained its prooxidant effect at all ratios tested. Similar results were obtained when varying ratios of ADP to Fe(II) (Fig. 7B) were evaluated, with ADP enhancing the rates of LUV peroxidation at all concentrations tested. Citrate, on the other hand, reversed its prooxidant effect at higher chelator concentrations in the presence of both Fe(II) (Fig. 7C) and Fe(III) ions (Fig. 7D). With Fe(II) ions, citrate did not exhibit any antioxidant activity up to a chelator-to-metal molar ratio of 5:1. At chelator-to-Fe(III) molar ratios of 10:1 and 20:1, though, citrate strongly suppressed peroxidation in the LUV, as evidenced by the small drop in intensity over the assay period. In the presence of Fe(III) ions, citrate reversed its prooxidant effect at chelator-to-metal ratios of 5:1 and higher.

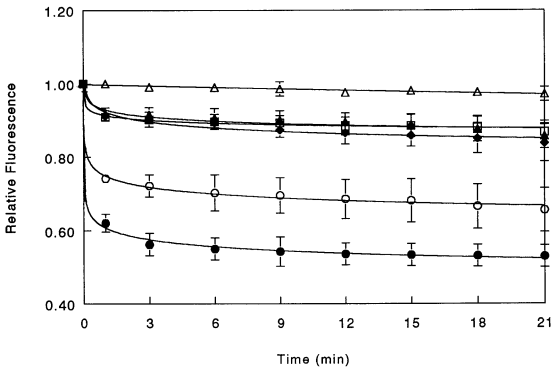

FIG. 5. Peroxidation of 100 μM SLPC LUV induced by 1 μM Fe(III) and 2 μM chelator. The rate of peroxidation was monitored by a decrease in fluorescence intensity as a function of time, as described in the Experimental Procedures section. Relative fluorescence on the y-axis represents the ratio of fluorescence intensity after a given time of oxidation vs. initial intensity at time = 0 min. Values represent the mean ± standard deviation of triplicate measurements; △, control; ○, Fe(III); □, Fe(III)-EDTA; ◆, Fe(III)-ADP; ▲, Fe(III)-NTA; ●, Fe(III)-citrate. See Figures 1 and 3 for abbreviations.

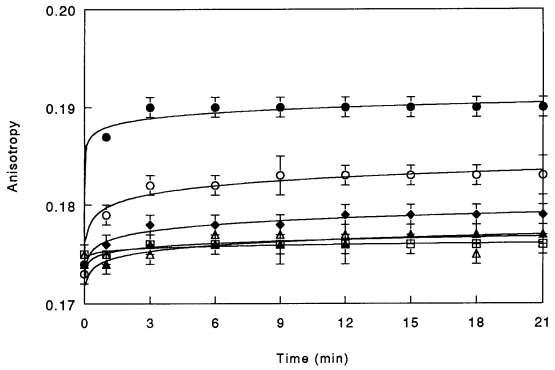

FIG. 6. Peroxidation of 100 μM SLPC LUV induced by 1 μM Fe(III) and 2 μM chelator. The rate of peroxidation was followed by an increase in fluorescence anisotropy as a function of time, as described in the Experimental Procedures section. Values represent the mean ± standard deviation of triplicate measurements; △, control; ○, Fe(III); □, Fe(III)-EDTA; ◆, Fe(III)-ADP; ▲, Fe(III)-NTA; ●, Fe(III)-citrate. See Figures 1 and 3 for abbreviations.

Validation of the fluorescence-based assays. Quantitation of conjugated diene and hydroperoxide formation as a function of time was done by HPLC to establish the validity of the fluorescence intensity and anisotropy measurements in the model system as assays for lipid peroxidation. The data in Figures 8 and 9 show the amounts of conjugated dienes and phosphatidylcholine hydroperoxides (PCOOH), respectively, that were formed during the Fe(II)-induced peroxidation of SLPC vesicles over a 90-min period. The PCOOH were specifically detected by chemiluminescence as a single peak that eluted at 6.5 min. By ultraviolet detection at 234 nm, an unoxidized PC peak was seen at 3.7 min and an oxidized PC peak at 6.4 min. Formation of conjugated dienes and PCOOH were consistent with the peroxidation measurements by fluorescence. At a chelator-to-metal molar ratio of 2:1, citrate caused the greatest acceleration of Fe(II)-induced formation of conjugated dienes and PCOOH in the LUV, followed by NTA and ADP. EDTA strongly suppressed the Fe(II)-induced formation of conjugated dienes and PCOOH.

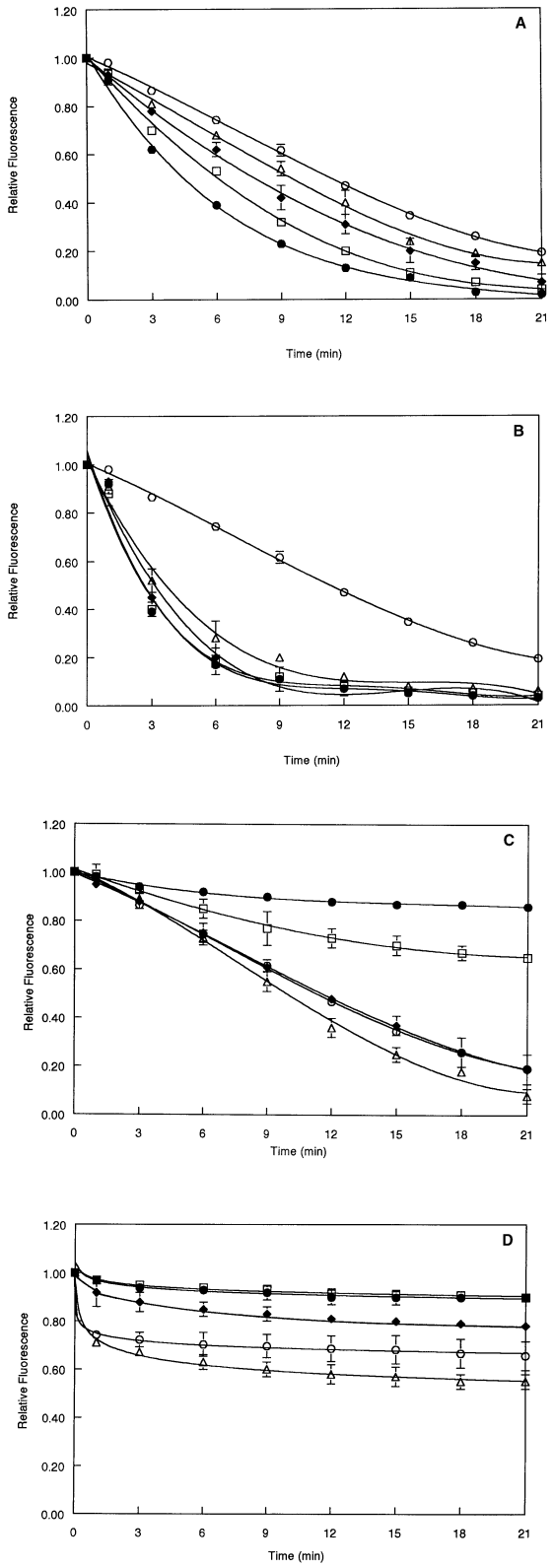

FIG. 7. Peroxidation of the LUV induced by varying molar ratios of (A) NTA to Fe(II), (B) ADP to Fe(II), (C) citrate to Fe(II) or (D) citrate to Fe(III). The concentration of metal was kept constant at 1 μM (○), and different concentrations of chelators were used for final chelator-to-metal molar ratios of 1:1 (△), 5:1 (◆), 10:1 (□) and 20:1 (●). Values represent the mean ± standard deviation of triplicate measurements. See Figures 1 and 3 for abbreviations.

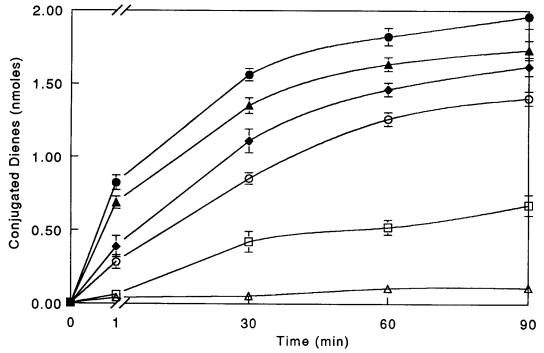

FIG. 8. Peroxidation of 2 mM SLPC LUV induced by 200 μM Fe(II) and 400 μM chelator. The rate of peroxidation was monitored by the measurement of conjugated diene absorption at 234 nm, as described in the Experimental Procedures section. Values represent the mean ± standard deviation of triplicate measurements; △, control; ○, Fe(II); □, Fe(II)-EDTA; ◆, Fe(II)-ADP; ▲, Fe(II)-NTA; ●, Fe(II)-citrate. See Figures 1 and 3 for abbreviations.

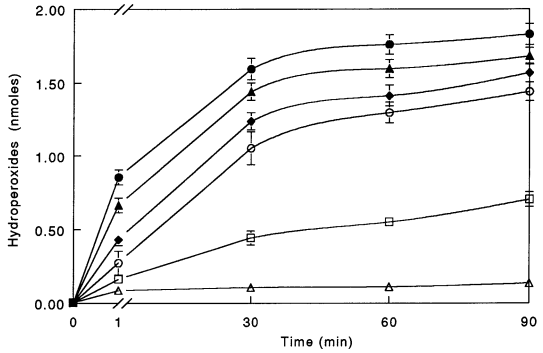

FIG. 9. Peroxidation of 2 mM SLPC LUV induced by 200 μM Fe(II) and 400 μM chelator. The rate of peroxidation was monitored by quantitation of hydroperoxides by high-performance liquid chromatography-chemiluminescence as described in the Experimental Procedures section. Values represent the mean ± standard deviation of triplicate measurements; △, control; ○, Fe(II); □, Fe(II)-EDTA; ◆, Fe(II)-ADP; ▲, Fe(II)-NTA; ●, Fe(II)-citrate. See Figures 1 and 3 for abbreviations.

DISCUSSION

Fluorescence spectroscopy has previously been used successfully to monitor lipid peroxidation in submitochondrial particles (28), low-density lipoproteins (29), microsomes (30), human erythrocyte membranes (15,31), and phospholipid vesicles (32). However, the probe used in these studies, *cis*-parinaric acid, requires special handling, has a relatively low quantum yield in membranes, and is subject to complicating photochemical and oxidative reactions, including dimerizations (33). DPH–PA overcomes these disadvantages and, therefore, offers great potential as a probe for membrane studies.

DPH–PA (Scheme 1) is an anionic derivative of the parent DPH molecule. In contrast to DPH, which is nonspecifically partitioned in various domains of the membrane (34), the

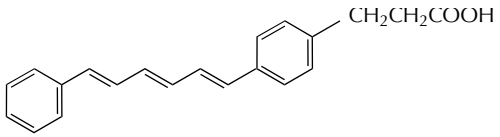

SCHEME 1

polar substituent of DPH–PA provides a surface anchor that ensures that the polar head of the probe is localized at the lipid–water interface of the membrane, with the hydrophobic tail portion lying parallel to the acyl chains of the membrane. In addition, the probe is similar to long-chain free fatty acids, both in its anionic carboxylic group and in its approximate chainlength, making it a useful probe for lipid peroxidation studies. The probe also lacks the extrinsic bulk of some other membrane probes, such as the *n*-(9-anthroyloxy) free fatty acid and pyrene derivatives, and can be expected to cause minimal disturbance to the lipid bilayer (35). In contrast to *cis*-parinaric acid, DPH–PA is relatively photostable and requires little special handling, exhibits strong fluorescence enhancement in a lipid environment, and offers sensitive fluorescence anisotropy responses to lipid ordering (36).

These favorable properties of the probe DPH–PA were utilized in developing fluorescence intensity and anisotropy assays for monitoring lipid peroxidation in membranes. The basis for the fluorescence intensity assay is the structure of the DPH–PA molecule, its conjugated double-bond system giving rise to its fluorescent properties, as well as to its susceptibility to peroxidation. The probe reacts readily with a variety of free radicals to yield nonfluorescent products. Degradation of the probe that accompanies membrane peroxidation is indicated by a decrease in fluorescence, which can then be measured directly. In contrast, the fluorescence anisotropy assay developed here follows the changes in membrane structure that accompany peroxidation. Free radical reactions such as lipid peroxidation have been implicated in decreased membrane fluidity (37,38). A decrease in membrane fluidity is indicated by an increase in the steady-state fluorescence anisotropy parameter of the probe.

The two fluorescence-based assays developed in this study were used to explore the effects of chelators on metal-ion-induced peroxidation. Of the three metal ions tested, Fe(II) ions caused the greatest acceleration of peroxidation in the liposomes, followed by Fe(III) ions. By contrast, Cu(II) ions were unable to induce peroxidation under the conditions used in this assay.

These differences in the abilities of the three metal ions to initiate peroxidation in the LUV are probably a result of the differences in accessibility of these oxidizing species to the site of peroxidation in the membranes. Cu(II) ions have previously been shown to be less effective at initiating lipid peroxidation in liposomes as compared to micelles (39). These researchers found that liposomal peroxidation by Cu(II) occurred after an initial lag phase during which peroxidation did not take place, suggesting that a physical constraint had to be overcome before massive lipid peroxidation could occur. When the lipid organization was shifted from bilayer to micellar dispersion, this lag phase was abolished.

The different coordination geometry of Cu(II) and Cu(I) also may affect their ability to participate in redox reactions of lipid peroxidation. Cu (II) complexes have a square planar geometry, whereas Cu(I) complexes are mostly tetrahedral. On the other hand, both Fe(II) and Fe(III) complexes are almost always octahedral or distorted octahedral. The fact that the two valence states of copper usually have different coordination environments may impose a kinetic hindrance on redox reactions involving copper (40).

Another factor that may explain the ability of iron and the inability of copper to initiate peroxidation in our system may be the different mechanisms through which these compounds catalyze lipid peroxidation. The presence of hydroperoxides is essential for a peroxidative response to copper, suggesting that copper catalyzes the degradation of lipid hydroperoxides and thus promotes the propagation phase of the peroxidation mechanism (41). Iron functions in both the initiation and propagation phases of lipid peroxidation (42). Because the lipid used in this study was of high purity and contained no detectable amounts of hydroperoxides, it may explain why Cu(II) was unable to initiate peroxidation in this liposomal system.

The two valence states of iron gave different rates of peroxidation and also showed different effects in the presence of chelators. Fe(II) ions caused greater acceleration of lipid peroxidation than did Fe(III) ions. A possible explanation for this difference in activity for the two metal ions is that only Fe(II) ions are active in peroxide decomposition, and although the system is seemingly pure, it is probable that trace peroxides and trace Fe(II) are responsible for much of the small peroxidation seen with Fe(III) ions.

All chelators examined in this study had a marked effect on the rates of metal-ion-induced peroxidations. Depending on the concentration of the chelator and on the metal ion used for peroxidation, these chelators either suppressed or promoted the rates of peroxidation. EDTA was an effective antioxidant in this system, irrespective of the valence state of iron used as the initiator of peroxidation. NTA and ADP, on the other hand, behaved as antioxidants in the presence of Fe(III) ions, but were prooxidants in the presence of Fe(II) ions. They maintained their prooxidant effect, even at the higher concentrations of chelators tested. In contrast, citrate displayed a prooxidant effect in the presence of Fe(II) and Fe(III) at the lower concentrations of chelators tested. However, when the concentration of chelators was in high molar excess over that of the metal ions, the prooxidant effect of citrate was reversed and it became an effective antioxidant.

This biphasic, paradoxical behavior of citrate may be attributed to the fact that, at the lower concentrations, citrate may be preferentially complexing the oxidized form of iron, leaving traces of the lower valence form in solution to participate in the Haber-Weiss reaction, reductively activating peroxides through formation of the hydroxide ion and the extremely reactive alkoxyl or hydroxyl free radicals (43). This

also would explain the promotion of citrate to antioxidant status, at the higher concentrations, when all of the iron would be chelated. Because one would expect citrate to be in much greater preponderance to the metal in a real food or biological system, the antioxidant activity of citrate would be the predominant one observed.

Another factor that may explain the different effects of the chelators studied on the rates of metal-catalyzed lipid peroxidation may be their effect on the redox potential of the metal ions. Transition metals have a range of accessible oxidation states that enables them to transfer electrons. The redox potential for such a transfer is altered by chelation of the metals (44). The reduction potential of Fe(III)/Fe(II) (aqueous) is +110 mV at pH 7.0. The reduction potential of the chelated Fe(III)EDTA/Fe(II)EDTA increases to +120 mV, whereas those of the chelated Fe(III)citrate/Fe(II)citrate and Fe(III)ADP/Fe(II)ADP complexes decrease to +100 mV at neutral pH (45).

In general, chelators in which oxygen atoms ligate the metal tend to preferentially bind to the oxidized forms of iron or copper, thereby decreasing the redox potential of these metals. In contrast, chelators in which nitrogen atoms primarily bind the metal favor the reduced forms of iron and copper and tend to increase the redox potential of the metal (40). This alteration of reduction potential influences the reactions in which iron can participate, which in turn changes the yields of the different reactive oxygen species obtained during iron autooxidation.

Alteration in the accessibility of the metal ions to the site of peroxidation after complexation with the different chelators also can influence the ability of the metal to participate in lipid peroxidation. Because metal ions are present in the aqueous phase and catalysis of membrane peroxidation must occur at the phase interface or membrane surface, any chelator that increases the binding of the metal to the membrane will increase the catalytic effectiveness of the metal (46). Chelators like ADP are known to increase fatty acid solubilization of the metals, thereby placing the metal at the site of peroxidation and enhancing the rate of lipid peroxidation (47). Other factors, such as the charge on the chelator and the steric effects of the complex formed, also can influence the rate of peroxidation. The net effect on lipid peroxidation often results from a complex competition between the individual effects (1).

Numerous other studies have demonstrated the complexity imparted by chelators on the reactivity of metals in lipid peroxidation. Chelators have variously been shown to have a prooxidant, antioxidant, or no effect on lipid peroxidation, depending on the source and preparation of tissues, cells, membranes or purified lipids, the solvents used, the concentrations of metal complexes, the presence or absence of oxygen sources, and also, how these effects are measured (1).

This illustrates the need of working with a clean and simple model system that is free from other complicating factors to better elucidate the molecular bases of these reactions. The SLPC lipid substrate used in this model system has a composition that is representative of the phospholipids found in biological membranes, with a saturated fatty acid at the *sn*-1 position, an unsaturated fatty acid at the *sn*-2, and a phosphate-containing polar group at the *sn*-3 position (48). The defined composition and high purity of this lipid also offered other obvious advantages. Because the model system was free of contaminating endogenous pro- or antioxidants, associated with biologically derived materials, and extreme care was taken to keep the system free from oxygen and metal contaminants until the time of initiation of oxidation, interpretations of the effects of chelators on membranal metal-induced peroxidation were subject to fewer ambiguities.

The results of the fluorescence studies that characterized the effects of chelators on Fe(II)-induced peroxidation were compared with the rates of PCOOH and conjugated diene formation, for validation of the fluorescence assays. The HPLC data showed that both hydroperoxides and conjugated dienes increased in concert with the rates of decrease in fluorescence intensity and membrane fluidity. This was strong evidence to support our hypothesis that the fluorescence changes observed upon the initiation of peroxidation stem from the metal-ion-induced generation of free radicals.

The fluorescence assays are especially useful in monitoring the initial stages of lipid peroxidation. The advantages of the fluorescence assays include extremely high sensitivity (<1 μmol of pure lipid is required to run an assay), the small concentration of probe required relative to lipid (ratio of probe molecules to lipid molecules is 1:350) so that the overall composition of the membrane is not significantly altered, and the low quantum yield of DPH–PA in water, ensuring that the measured fluorescence is emanating from within the membrane and not from the surrounding aqueous environment. In addition, these assays offer the speed of other accelerated tests, while avoiding the artifacts introduced by the high-temperature-abuse conditions.

The complexity and variability of food systems and biological materials preclude the use of any single method to define antioxidant activity. However, the experimental system developed here offers a promising alternative as a screening tool to evaluate antioxidant efficacy of purified compounds or plant extracts on membrane lipids prior to long-term studies in foods or in biological systems.

ACKNOWLEDGMENTS

The authors gratefully acknowledge the support of Michigan Agricultural Experiment Station and the M.S.U. Crop and Food Bioprocessing Center. They would also like to acknowledge Dr. J.I. Gray for helpful discussions on the manuscript and Dr. John Heckman for performing the SEM experiments.

REFERENCES

1. Schaich, K.M., Metals and Lipid Oxidation. Contemporary Issues, *Lipids 27:*209–218 (1992).
2. Barclay, L.R.C., Model Biomembranes: Quantitative Studies of Peroxidation, Antioxidant Action, Partitioning, and Oxidative Stress, *Can. J. Chem. 71*:1–16 (1993).

3. Braughler, J.M., R.L. Chase, and J.F. Pregenzer, Oxidation of Ferrous Iron During Peroxidation of Lipid Substrates, *Biochim. Biophys. Acta 921:*457–464 (1987).
4. Aust, S.D., L.A. Morehouse, and C.E. Thomas, Role of Metals in Oxygen Radical Reactions, *J. Free Radicals Biol. Med. 1:*3–25 (1985).
5. Spear, N., and S.D. Aust, Thiol-Mediated NTA-Fe(III) Reduction and Lipid Peroxidation, *Arch. Biochem. Biophys. 312:*198–202 (1994).
6. Tampo, Y., S. Onodero, and M. Yonaha, Mechanism of the Biphasic Effect of Ethylenediaminetetraacetate on Lipid Peroxidation in Iron-Supported and Reconstituted Enzymatic System, *Free Radicals Biol. Med. 17:*27–34 (1994).
7. Yoshida, Y., S. Furuta, and E. Niki, Effects of Metal Chelating Agents on the Oxidation of Lipids Induced by Copper and Iron, *Biochim. Biophys. Acta 1210:*81–88 (1993).
8. Dikalov, S., P. Alov, and D. Rangelova, Role of Iron Ion Chelation by Quinones in Their Reduction, OH-Radical Generation and Lipid Peroxidation, *Biochem. Biophys. Res. Commun. 195:*113–119 (1993).
9. Miller, D.M., N.H. Spear, and S.D. Aust, Effects of Deferrioxamine on Iron-Catalyzed Lipid Peroxidation, *Arch. Biochem. Biophys. 295:*240–246 (1992).
10. Fujii, T., Y. Hiramoto, J. Terao, and K. Fukuzawa, Site-Specific Mechanisms of Initiation by Chelated Iron and Inhibition by α-Tocopherol of Lipid Peroxide-Dependent Lipid Peroxidation in Charged Micelles, *Ibid. 284:*120–126 (1991).
11. Frankel, E.N., In Search of Better Methods to Evaluate Natural Antioxidants and Oxidative Stability in Food Lipids, *Trends Food Sci. Technol. 4:*220–225 (1993).
12. Monahan, F.J., J.I. Gray, A. Asghar, A. Haug, G.M. Strasburg, D.J. Buckley, and P.A. Morrissey, Influence of Diet on Lipid Oxidation and Membrane Structure in Porcine Muscle Microsomes, *J. Agric. Food Chem. 42:*59–63 (1994).
13. Dinis, T.C.P., L.M. Almeida, and V.M.C. Madeira, Lipid Peroxidation in Sarcoplasmic Reticulum Membranes: Effect on Functional and Biophysical Properties, *Arch. Biochem. Biophys. 301*:256–264 (1993).
14. Tien, M.T., B.A. Svingen, and S.D. Aust, An Investigation into the Role of Hydroxyl Radical in Xanthine Oxidase-Dependent Lipid Peroxidation, *Ibid. 216:*142–151 (1982).
15. McKenna, R., F.J. Kedzy, and D.E. Epps, Kinetic Analysis of the Free-Radical-Induced Lipid Peroxidation in Human Erythrocyte Membranes: Evaluation of Potential Antioxidants Using *cis*-Parinaric Acid to Monitor Lipid Peroxidation, *Anal. Biochem. 196:*443–450 (1991).
16. Thomas, J.P., M. Maiorino, F. Ursini, and A.W. Girotti, Protective Action of Phospholipid Hydroperoxide Glutathione Peroxidase Against Membrane-Damaging Lipid Peroxidation, *J. Biol. Chem. 265:*454–461 (1990).
17. Svingen, B.A., J.A. Buege, F.O. O'Neil, and S.D. Aust, The Mechanism of NADPH-Dependent Lipid Peroxidation. The Propagation of Lipid Peroxidation, *Ibid. 254*:5892–5899 (1979).
18. Kanner, J., B. Hazan, and L. Doll, Catalytic "Free Iron" in Muscle Foods, *J. Agric. Food Chem. 36:*412–415 (1988).
19. Kellogg, E.W., III, and I. Fridovich, Superoxide, Hydrogen Peroxide, and Singlet Oxygen in Lipid Peroxidation by a Xanthine Oxidase System, *J. Biol. Chem. 250:*8812–8817 (1975).
20. Girotti, A.W., and J.P. Thomas, Superoxide and Hydrogen Peroxide-Dependent Lipid Peroxidation in Intact and Triton-Dispersed Erythrocyte Membranes, *Biochem. Biophys. Res. Commun. 118*:474–480 (1984).
21. Vigo-Pelfrey, C., and N. Nguyen, Modulation of Lipid peroxidation of Liposomes and Micelles by Antioxidants and Chelating Agents, in *Membrane Lipid Oxidation,* vol. II, edited by C.Vigo-Pelfrey, CRC Press, Boca Raton, 1991, pp. 135–149.
22. Strasburg, G.M., and R.D. Ludescher, Theory and Applications of Fluorescence Spectroscopy in Food Research, *Trends Food Sci. Technol. 6:*69–75 (1995).
23. MacDonald, R.C., R.I. MacDonald, B.P.M. Menco, K. Takeshita, N.K. Subbarao, and L. Hu, Small-Volume Extrusion Apparatus for Preparation of Large, Unilamellar Vesicles, *Biochim. Biophys. Acta 1061:*297–303 (1991).
24. Lakowicz, J.R., in *Principles of Fluorescence Spectroscopy,* Plenum Press, New York, 1983, pp. 111–150.
25. Miyazawa, T., K. Yasuda, and K. Fujimoto, Chemiluminescence–High Performance Liquid Chromatography of Phosphatidylcholine Hydroperoxide, *Anal. Letters 20:*915 (1987).
26. Zhang, J.-R., A.R. Cazers, B.S. Lutzke, and E.D. Hall, HPLC–Chemiluminescence and Thermospray LC/MS Study of Hydroperoxides Generated from Phosphatidylcholine, *Free Radicals Biol. Med. 18:*1–10 (1995).
27. Jiang, Z.-Y., A.C.S. Woollard, and S.M. Wolff, Lipid Hydroperoxide Measurement by Oxidation of Fe^{2+} in the Presence of Xylenol Orange. Comparison with the TBA Assay and an Iodometric method, *Lipids 26:*853–856 (1991).
28. de Hingh, Y.C.M., J. Meyer, J.C. Fischer, R. Berger, J.A.M. Smeitink, and J.A.F. Op den Kamp, Direct Measurement of Lipid Peroxidation in Submitochondrial Particles, *Biochemistry 34:*12755–12760 (1995).
29. Laranjinha, J.A.N., L.M. Almeida, and V.M.C. Madeira, Lipid Peroxidation and Its Inhibition in Low Density Lipoproteins: Quenching of *cis*-Parinaric Acid Fluorescence, *Arch. Biochem. Biophys. 297:*147–154 (1992).
30. Dinis, T.C.P., V.M.C. Madeira, and L.M. Almeida, Action of Phenolic Derivatives (Acetaminophen, Salicylate, and 5-Aminosalicylate) as Inhibitors of Membrane Lipid Peroxidation and as Peroxyl Radical Scavengers, *Ibid. 315:*161–169 (1994).
31. Van den Berg, J.J.M., F.A. Kuypers, J.H. Oju, D. Chiu, B. Lubin, B. Roelefsen, and J.A.F. Op den Kamp, The Use of *cis*-Parinaric Acid to Determine Lipid Peroxidation in Human Erythrocyte Membranes. Comparison of Normal and Sickle Erythrocyte Membranes, *Biochim. Biophys. Acta 944:*29–39 (1988).
32. Kuypers, F.A., J.J.M. Van den Berg, C. Schalkwijk, B. Roelofsen, and J.A.F. Op den Kamp, Parinaric Acid as a Sensitive Fluorescent Probe for the Determination of Lipid Peroxidation, *Ibid. 921:*266–274 (1987).
33. Lentz, B.R., Use of Fluorescent Probes to Monitor Molecular Order and Motions Within Liposome Bilayers, *Chem. Phys. Lipids 64:*99–116 (1993).
34. Ivessa, E.N., E. Kalb, F. Paltauf, and A. Hermetter, Diphenylhexatrienyl Propanoyl Hydrazyl Stachyose: A New Oligosaccharide Derivative of Diphenylhexatriene. Synthesis and Fluorescence Properties in Artificial Membranes, *Ibid. 49:*185–195 (1988).
35. Trotter, P.J., and J. Storch, 3-[*p*-(6-Phenyl)-1,3,5-hexatrenyl)-phenylpropionic acid (PA–DPH): Characterization as a Fluorescent Membrane Probe and Binding to Fatty Acid Binding Proteins, *Biochim. Biophys. Acta 982:*131–139 (1989).
36. Mateo, C.R., M.P. Lillo, J. Gonzalez-Rodriguez, and A.V. Acuna, Molecular Order and Fluidity of the Plasma Membrane of Human Platelets from Time-Resolved Fluorescence Polarization, *Eur. Biophys. J. 20:*41–52 (1991).
37. Yu, B.P., E.A. Suescun, and S.Y. Yang, Effect of Age-Related Lipid Peroxidation on Membrane Fluidity and Phospholipase A_2: Modulation by Dietary Restriction, *Mech. Age. Dev. 65:*17–33 (1992).
38. Choe, M., C. Jackson, and B.P. Yu, Lipid Peroxidation Contributes to Age-Related Membrane Rigidity, *Free Radicals Biol. Med. 18*:977–984 (1995).
39. Maiorino, M., A. Zamburlini, A. Roveri, and F. Ursini, Copper-Induced Lipid Peroxidation in Liposomes, Micelles, and LDL: Which Is the Role of Vitamin E, *Ibid. 18:*67–74 (1995).

40. Miller, D.M., G.R. Buettner, and S.D. Aust, Transition Metals as Catalysts of "Autoxidation" Reactions, *Ibid. 8:*95–108 (1990).
41. Ding, A.-H., and P.C. Chan, Singlet Oxygen in Copper-Catalyzed Lipid Peroxidation in Erythrocyte Membranes, *Lipids 19*:278–284 (1984).
42. Minotti, G., Sources and Role of Iron in Lipid Peroxidation, *Chem. Res. Toxicol. 6:*134–146 (1993).
43. Porter, W.L., Paradoxical Behavior of Antioxidants in Food and Biological Systems, *Toxicol. Indust. Health 9:*93–122 (1993).
44. Kanner, J., J.B. German, and J.E. Kinsella, Initiation of Lipid Peroxidation in Biological Systems, *CRC Crit. Rev. Food Sci. Nutr. 25*:317–364 (1987).
45. Buettner, G.R., The Pecking Order of Free Radicals and Antioxidants: Lipid Peroxidation, α-Tocopherol, and Ascorbate, *Arch. Biochem. Biophys. 300:*535–543 (1993).
46. Willson, R.L., Iron and Hydroxyl Free Radicals in Enzyme Inactivation and Cancer, in *Free Radicals, Lipid Peroxidation, and Cancer,* edited by D.C.H. McBrien and T.F. Slater, Academic Press, London, 1982, pp. 275–303.
47. Schaich, K.M., and D.C. Borg, Fenton Reactions in Lipid Phases, *Lipids 23:*570–579 (1988).
48. Stanley, D.W., Biological Membrane Deterioration and Associated Quality Loss in Food Tissues, *CRC Crit. Rev. Food Sci. Nutr. 30:*487–553 (1991).

[Received May 23, 1996; accepted July 7, 1997]